# Dynamic and Steady-State Rheological Measurements on Polymer Melts

R. M. SCHULKEN, R. H. COX, and L. A. MINNICK, *Research Laboratories, Tennessee Eastman Company, Division of Eastman Kodak Company, Kingsport, Tennessee 37662*

## Synopsis

Many attempts to correlate steady-state and dynamic rheological data have been reported. Thus far, the correlations have not been convincing, particularly for polymer melts that exhibit highly non-Newtonian behavior. The purpose of this work was to provide a means for obtaining a useful correlation. The Maxwell viscoelastic model was used to correlate data from four different modes of shear—two involving steady-state deformation and two involving dynamic deformation. As certain defined requirements were met, excellent agreement was obtained for polymer melts that represent a wide range of viscoelastic behavior. One of these requirements was that the polymer molecule should have a certain degree of flexibility.

## INTRODUCTION

The flow behavior of polymer melts and solutions is usually determined by steady-state deformation measurements made on capillary-extrusion or rotating-disk instruments. These measurements are useful because they are convenient and they simulate closely the flow character of polymer melts in commercial processes. However, these measurements are disadvantageous in at least two respects: separating the viscous and elastic components of deformation is difficult, and the range of shear rates available is insufficient for adequate characterization.

Oscillation, or dynamic, measurements provide an easy means of separating the viscous and elastic components of polymer melts and of determining shear rates of $<10^{-2}$ to $>10^{2}$ rad/sec. Measurements at these low rates of deformation and measurements of the elastic as well as the viscous polymer melt flow components are very important in characterizing the polymers used in many applications. These low rates also provide data that are useful for molecular and morphological characterization.

No generally accepted method exists for correlating steady-state and dynamic rheological data. Reports show that attempts have been made to correlate steady-state viscosity with the viscous, or loss, component of the complex viscosity ($\eta'$), the absolute value of the complex viscosity [$\eta^*$] (the Cox–Merz correlation), and the viscosity in the Maxwell element; but the data presented thus far have not been convincing, particularly for melts that exhibit highly non-Newtonian behavior. The purpose of this work was to provide a means for obtaining a useful correlation.

For this work, we chose four different but commonly used methods for determining rheological behavior characteristics. These included two steady-state methods—one that used the Instron capillary viscometer and one that used the

Journal of Applied Polymer Science, Vol. 25, 1341–1353 (1980)

0021-8995/80/0025-1341$01.30

Rheometrics Mechanical Spectrometer rotation of cone and plate—and two dynamic methods—both of which used the Mechanical Spectrometer (with the cone and plate oscillating in rotation and with eccentric rotating disks). For comparison we chose a number of different materials that represent a wide range of viscoelastic behavior.

Unfortunately, some problems are encountered in relating steady-state to dynamic data. One problem concerns the relationship between shear rate and angular frequency. In dynamic measurements the actual shear rate varies between a peak value and zero. This problem has been analyzed by a number of workers, and it is generally accepted that if the frequency is expressed in rad/sec and the amplitude of the oscillation is small, the numerical value is the same as the value for the steady-state shear rate expressed in $sec^{-1}$.[1] Bueche, Pao, and others have developed concepts to explain this agreement, but it should be validated for different types of tests and materials.

Another problem that arises in comparing dynamic and steady-state data involves the choice of a model for calculating material parameters from measured values. Real viscoelastic materials have a broad range of relaxation times. In calculating data from measured values, the usual practice is to assume that a particular relaxation time is appropriate to a particular frequency or shear rate. Measurements made over a range of frequencies permit the appropriate relaxation times to be determined; hence, the relaxation spectrum as well can be determined.

The single relaxation time assumed for a particular frequency has two Newtonian elements—a viscous element (dash pot with viscosity $\eta$) and an elastic element (spring with elastic modulus $G$). These elements may be assumed to be in parallel (Voigt or Kelvin model, where stresses are added) or in series (Maxwell model, where strains are added). The relaxation time ($\tau$) is $\eta/G$, the time required in a series or Maxwell system for an applied stress to decay to its original value divided by $e$. The relaxation spectrum is simulated by a number of Voigt elements in series or by a number of Maxwell elements in parallel, and the results are identical.

The equations for these models can be written as follows:

$$\text{Voigt} \qquad S = G_v\gamma + \eta_v\dot{\gamma}$$

$$\text{Maxwell} \qquad \dot{\gamma} = S/\eta_m + \dot{S}/G_m$$

where $S$ and $\gamma$ are the stress and the strain, the dot signifies the derivative with respect to time (i.e., $\dot{\gamma} = d\gamma/dt$), and the subscripts are $v$ for Voigt and $m$ for Maxwell.

Experience has shown that the viscous and elastic parameters are constant if the frequency (or shear rate), the temperature, and the shear history are constant. Thus, in most conventions the data are presented as plots of $\eta$ and $G$, or some similar single parameters as functions of frequency or temperature, or by superposition of $\omega$ and temperature to form a master curve. In these cases, the right choice of model will be determined by its purpose.

Our purpose was to correlate data from four different measuring techniques. It is obvious that a single Voigt model can respond as either a fluid or a solid in oscillatory testing under limited strain; but in a steady-state deformation the Voigt model cannot give a normal fluid response if the elastic component is significant, since the stress will increase with strain as well as with $\dot{\gamma}$. Conversely,

a single Maxwell model can respond as a fluid in either an oscillatory or a steady-state deformation. The Voigt model is usually chosen for solidlike behavior because of its characteristic small deformation of a damped or retarded spring. The Voigt model may also be applicable to certain transitory behavior of fluids. The Maxwell model is most useful for liquids or melts because of its characteristic of being able to undergo infinite deformation with partial elastic recovery. Thus, for comparison of oscillatory data with steady-state data in such plots the single Maxwell model is more appropriate than the single Voigt model because a steady-state deformation must be Maxwellian, whereas dynamic or transitory deformation can be either Voigtian or Maxwellian.

The dynamic properties of fluids are commonly measured by using a cone-and-plate rheometer. One platen is oscillated in rotation, so that variations in shear strain as a function of time are described by a sine curve and an equation of the following form:

$$\gamma_t = \gamma_0 \sin(\omega_t)$$

where $\gamma_t$ is the strain at time $t$, $\gamma_0$ is the maximum amplitude of strain, and $\omega$ is the frequency of oscillation in rad/sec.

Then the rate of strain is as follows:

$$\dot{\gamma} = \gamma_0 \omega \cos(\omega_t)$$

The part of the stress that is in phase with the strain is related to the elastic response—the part in phase with the rate of strain is related to the viscous response. The actual stress then is shown by the following equation, where $\delta$ is the phase angle (0–90°) by which the stress leads the strain:

$$S_t = S_0 \sin(\omega + \delta)$$

These equations, combined with those for the Voigt and Maxwell models, yield the equations for calculating model parameters from dynamic data:

| Voigt | Maxwell |
|---|---|
| $G_v = (S_0/\gamma_0) \cos \delta = G'$ | $G_m = S_0/\gamma_0 \cos \delta$ |
| $\eta_v = (S_0/\gamma_0\omega) \sin \delta = \eta'$ | $\eta_m = S_0/\gamma_0\omega \sin \delta$ |
| $(S_0/\gamma_0) \sin\delta = G''$ | |

These equations are consistent with those of Ferry[1] and Benbow et al.[2] Note that the familiar dynamic parameters $G'$ and $\eta'$ are equivalent to the Voigt-model constants. The Voigt- and Maxwell-model equations are similar in form except that their trigonometric parts are reciprocally related. (Details of one method of derivation are shown in Appendix A.) These equations can be derived in a variety of ways, and equations can be derived for sinusoidal oscillation without recourse to a particular model. Then groups may be taken from these generalized equations to calculate material parameters. However, if the equation is essentially in the form of a summation of stresses, Voigt-type equations are obtained. The familiar $G^* = G' + iG''$ is an example. If the equation is in the form of a summation of strains or rates of strain, Maxwell-type equations are obtained.

A relatively new method for measuring dynamic properties of materials employs eccentric rotating disks (ERD). Bryce Maxwell suggested this method, and he and others developed it further. By this method, a sample fills a small gap between two disks with parallel faces that are free to rotate on the same axis, and the axis is perpendicular to the disk faces. One disk is driven in rotation and the other is free to rotate on a frictionless bearing (air).

Under these conditions, no force is generated on the freely rotating disk. However, if a slight offset in the axis is induced during rotation, a force will develop. The component of the force parallel to the direction of the offset, $F_x$, is proportional to the elastic component. The component of the force perpendicular to the direction of offset ($F_y$, parallel to the face) is proportional to the viscous component. The equations taken from the Rheometrics manual and Macosko[3] for calculating Voigt parameters are as follows:

$$G_v = F_x h/\pi R^2 a = G'$$

$$\eta_v = F_y h/\omega \pi R^2 a = \eta' = G''/\omega$$

$$\eta_v \omega/G_v = F_y/F_x = \tan\delta = \tau\omega$$

where $h$ is the distance between the disks, and $R$ is the radius of the disks.

Equations for calculating Maxwell parameters from ERD data can be derived by combining the equations for sinusoidal oscillation with the equations for the Voigt parameters. The equations for calculating Maxwell parameters are as follows:

$$G_m = \frac{F_x h}{\pi R^2 a \cos^2 \tan^{-1}(F_y/F_x)}$$

$$\eta_m = \frac{F_y h}{\omega \pi R^2 a \sin^2 \tan^{-1}(F_y/F_x)}$$

$$N_2/N_1 = F_z h/2F_y a$$

$$N_1 = 2S^2/G_m = (\eta_m \omega)^2 2/G_m$$

where $N_1$ and $N_2$ are the first and second normal-stress differences, and $F_z$ is the normal force measured during testing.

The ERD testing produces a massaging shear that has a number of advantages over normal oscillation. However, appropriate corrections for instrument compliance should be made as needed.

## EXPERIMENTAL

The capillary extrusion data were obtained by using an Instron capillary rheometer. Corrections were made for end effects, barrel resistance, and non-parabolic-flow profiles, where applicable. The rotational, oscillation, and ERD data were obtained by using a Rheometrics Mechanical Spectrometer and following normally prescribed methods. In all cases, the calibrations were made by measurement of geometric dimensions and by dead-weight calibration of force-measuring meters in the equipment, not by using a calibrating material such as a National Bureau of Standards fluid. Thus there were no arbitrary adjustable parameters or calibration constants. Corrections for instrument compliance and inertial effects were made as needed.

The specific materials used are described briefly in the discussion. Care was taken to minimize the effects of degradation and oxidation.

## DISCUSSION

Figure 1 shows the rheological data obtained from all four methods on a sample of Tenite 800 (Kodak) polyethylene. This low-density polyethylene is highly shear sensitive and viscoelastic; therefore, it represents a very stringent test of the correlation. This figure shows only three to four decades where the data from the different methods overlap. It is obvious that the dynamic values calculated by using the equations from the Maxwell model ($\eta_m$) correlate very well with the steady-state data: there are four different types of points on the same viscosity curve.

The Voigt-parameter plots ($\eta_v$) shown by the dashed curves occur at lower values, and they do not agree with the Maxwell parameters or the capillary data. Complex viscosity values lie about halfway between the Voigt and the Maxwell curves, thus not agreeing with either. To prevent clutter, data points are not shown on the Voigt curves; but the scatter would be similar to that of the Maxwell values, since the Voigt values are calculated from the same raw data. The fit of the data points plotted on the original drawing of this graph was better than the fit shown here.

Figure 2 compares data from testing "Bouncing Putty" silicone rheological material, a highly viscoelastic demonstrator sample supplied with the Rheometrics Mechanical Spectrometer. Insufficient sample was available for Instron testing, but the other three methods showed excellent agreement.

Figure 3 compares data from testing a copolymerization-modified poly(ethylene terephthalate) (PET). The data correlate well only for Maxwell-model calculations.

Figure 4 compares data from testing branched and modified PET. Branching was achieved by copolymerization with a few tenths percent of trifunctional acid. Again the Maxwell data correlate well.

Figure 5 compares these same linear and branched polyesters, which had about the same average melt viscosity and IV (inherent viscosity). These curves show the effect of branching. Note that the branched material is more shear sensitive

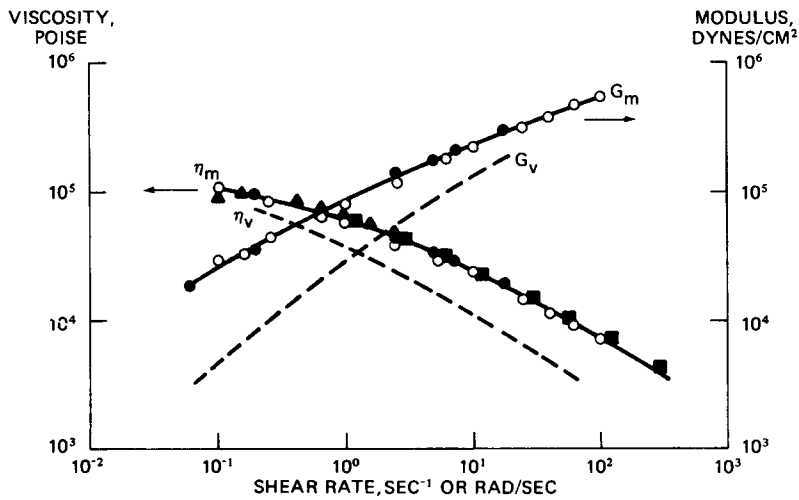


Fig. 1. Rheological properties of "Tenite" 800 polyethylene at 180°C; (○) RMS eccentric rotating disks (ERD); (▲) RMS cone + plate (steady state) (CPS); (●) RMS cone + plate (oscillation) (CPO); (■) Instron capillary rheometer.

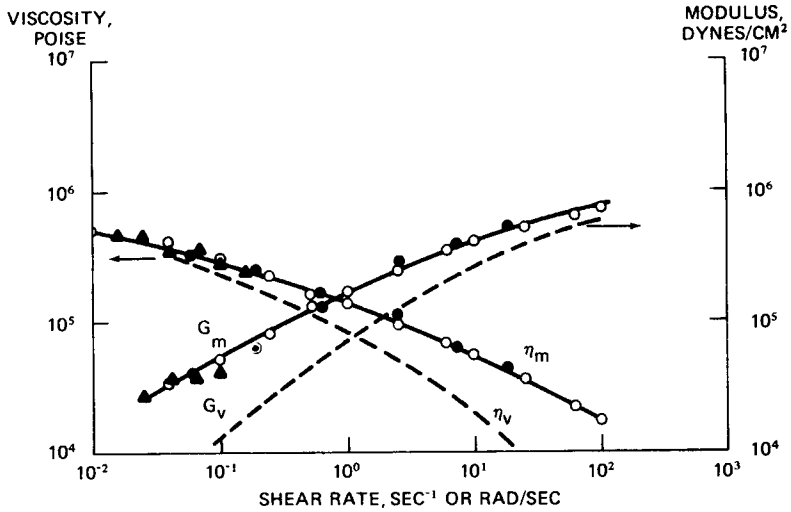


Fig. 2. Rheological properties of RMS demonstrator sample ("Bouncing Putty" silicone) at 24°C. Symbols as in Fig. 1.

and has a lower $G_m$, thus showing more elasticity, particularly at lower shear rates, or frequencies than the linear material.

Figure 6 compares Instron and ERD data on a sample of unmodified PET that is sensitive to degradation at temperatures required for rheological measurements. This melt is fairly Newtonian in behavior.

Figure 7 compares data from testing a liquid-crystal copolymer of PET and *p*-hydroxybenzoic acid. Note the approach to an upper Newtonian region not often seen in polymer melts. The low value of $G_m$ at low rates indicates a long relaxation time.

Other materials that give good agreement for the four methods include samples of bisphenol A polycarbonate and Delrin acetal thermoplastic.

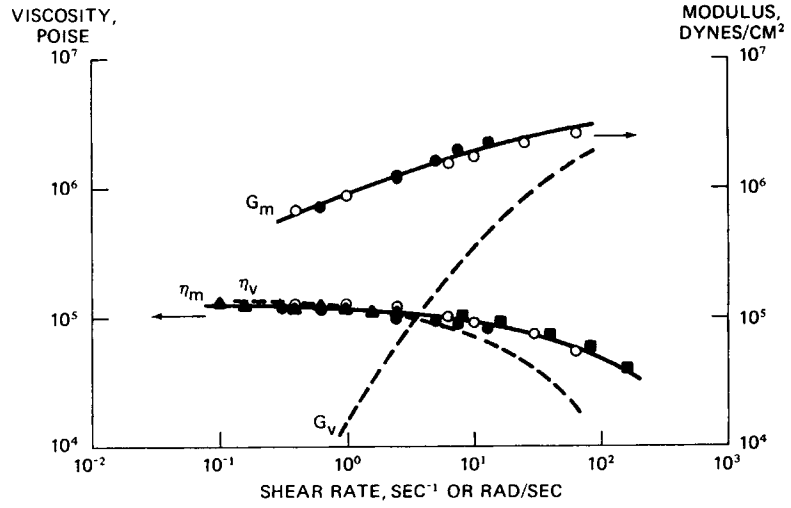


Fig. 3. Rheological properties of modified poly(ethylene terephthalate) at 200°C. Symbols as in Fig. 1.

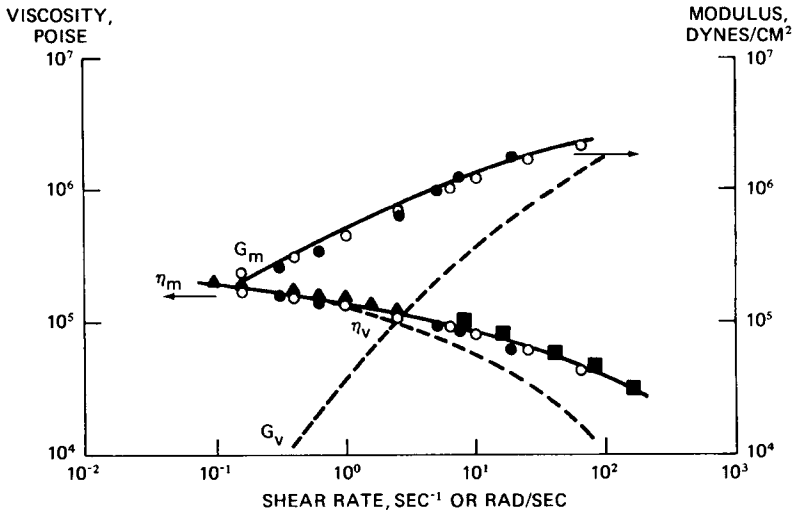


Fig. 4. Rheological properties of branched and modified poly(ethylene terephthalate) at 200°C. Symbols as in Fig. 1.

Figure 8 compares capillary and ERD viscosity values for two hot-melt adhesives. For sample A the data agree quite well. Data from the two methods do not agree for sample B. During capillary-extrusion testing on sample B, severe melt fracture occurred, particularly at high shear rates. This fracture mechanism reduced the extrusion force; thus the calculated values for the viscosity are spuriously low. This discrepancy, however, is expected. The test results indicate that measurements in the shear-rate region of melt fracture can be made more accurately by a dynamic method than by a steady-state method.

Figure 9 shows that the effect of strain amplitude on the calculated parameters is very small. Each tag on a data point shows the different amplitudes tested. The range was from a strain of 0.05 to 0.5.

The data presented thus far were obtained on materials that represent a wide

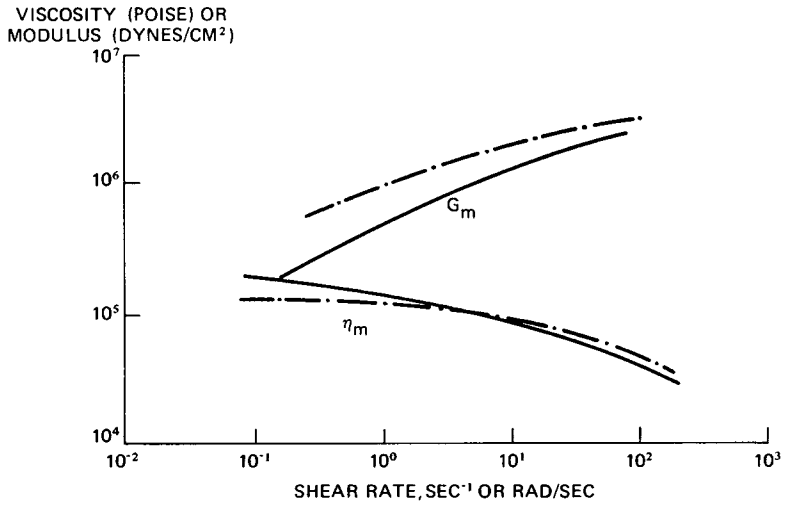


Fig. 5. Comparison of rheological properties of linear (—·—·—) and branched (——) polyesters.

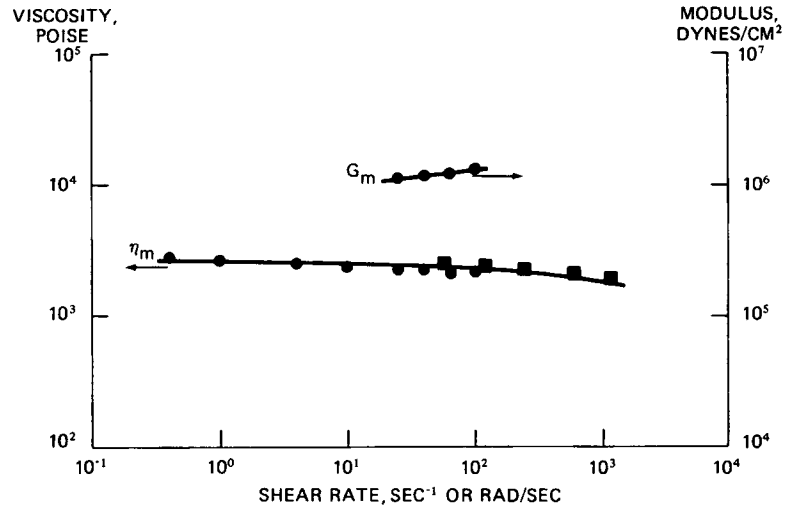


Fig. 6. Rheological properties of poly(ethylene terephthalate) at 285°C; (●) RMS eccentric rotating disks (ERD); (■) Instron capillary rheometer.

range of rheological behavior. Bueche[4] suggested that polymers composed of very stiff rodlike molecules may not give good agreement in comparing steady-state shear rate with dynamic frequency. The polymers discussed thus far in this work were composed of very flexible to only moderately stiff molecules. Characteristic ratios, a measure of chain stiffness, were seven or less. (The characteristic ratio is the ratio of the mean-square end-to-end distance of a molecule to the product of the number of bonds and the square of the bond length.)

Figure 10 compares capillary and ERD data for polystyrene, which is composed of fairly stiff molecules and has a characteristic ratio of about 10. No melt fracture was observed. The disagreement is obvious. The lower plot of capillary data falls about where a plot of the absolute value of the complex viscosity would lie. This may account for some of the correlations found in earlier work, since

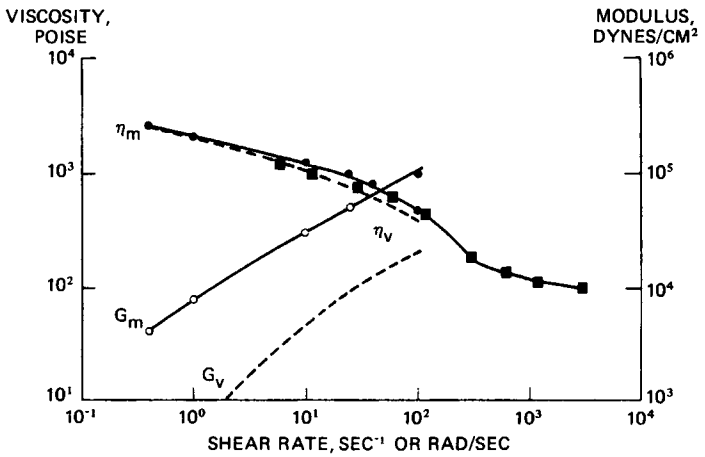


Fig. 7. Rheological properties of liquid-crystal polyester at 260°C. Symbols as in Fig. 6.

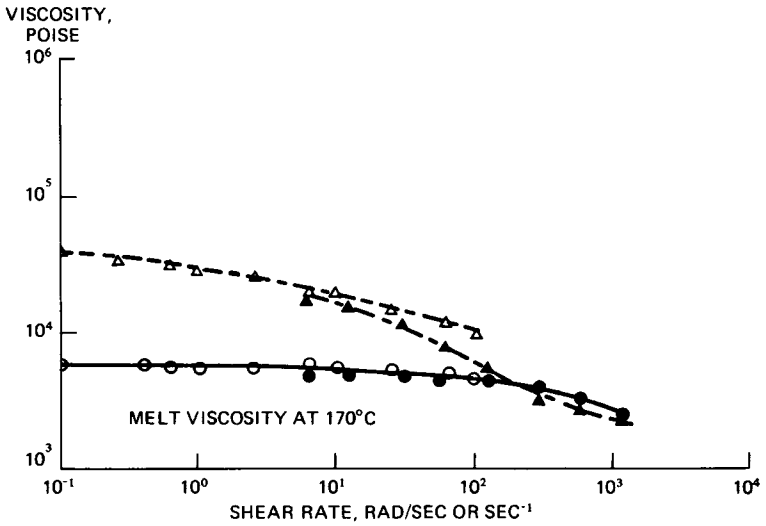


Fig. 8. Viscosities of two hot-melt adhesives; sample A(B), capillary extrusion ● (▲), ERD ○ (△).

polystyrene has been used extensively as a standard material for rheological measurements. Data for $\eta_v$ or $\eta'$ fall well below the capillary data.

Figure 11 shows test results for cellulose acetate butyrate, which has a characteristic ratio of about 15, indicating very stiff molecules. The discrepancy here is even greater than for polystyrene. Plots of $\eta^*$ and $\eta_v$ do not agree with any of the other data.

Plasticized cellulose acetate gave test results similar to those for cellulose acetate butyrate. It is obvious that the agreement breaks down for these stiff-molecular polymers. However, the largest disagreement is not between dynamic and steady-state flows but in the geometry of the flow. The capillary-flow data are much lower than the data from the other three methods. There was no ob-

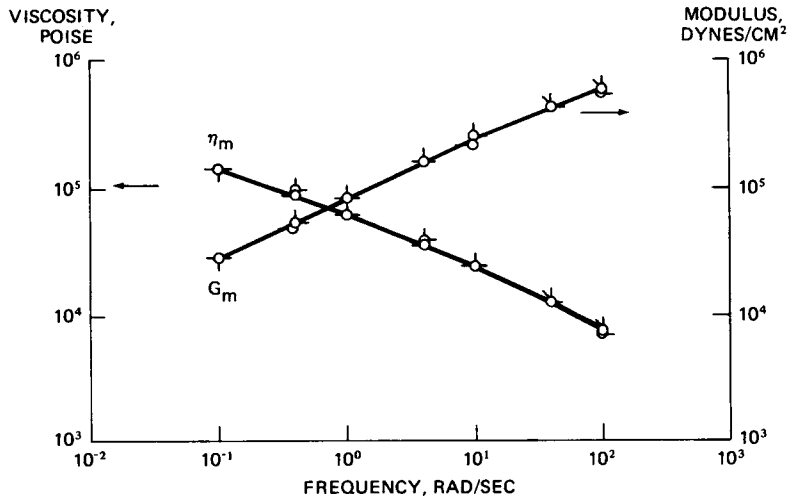


Fig. 9. Effect of strain amplitude on rheological properties of Tenite 800 polyethylene at 180°C. Strain amplitude: (○) 0.5; (○) 0.3; (○) 0.2; (○) 0.1; (○) 0.05.

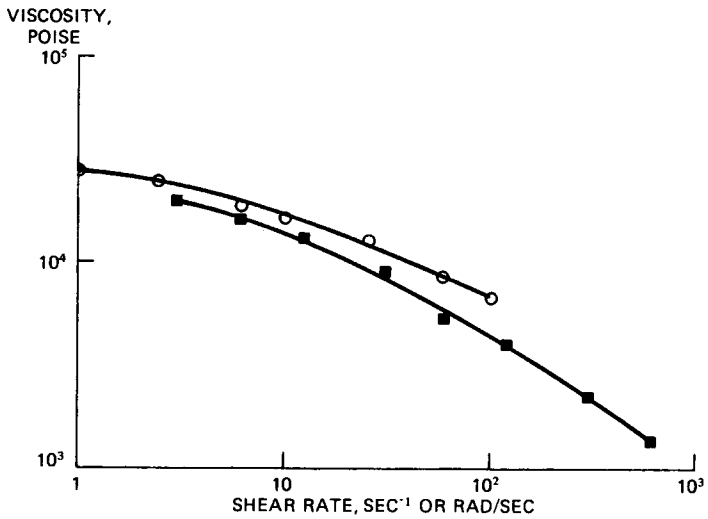


Fig. 10. Rheological properties of polystyrene at 240°C. Symbols as in Fig. 1.

vious melt fracture involved in the capillary testing, and the elongational part of the flow would not be expected to be significant because of the large length-to-diameter ratio ($L/D$ values of 7–160 were used). There is also a difference between ERD data and oscillating cone-and-plate data. Steady-state cone-and-plate data are close to oscillating cone-and-plate data. It does not appear that a simple horizontal shift on the $\omega$ axis would cause the data to agree.

A paper was recently published by Bonnebat and Devries[5] that gave poly(vinyl chloride) (PVC) dynamic and capillary data that agree by use of the Cox–Merz correlation. Our data on PVC agree with these results at frequencies below 60 rad/sec. At higher frequencies the dynamic and capillary data diverge. This agreement indicates behavior similar to that of polystyrene. The characteristic ratio of PVC is about 7.5, which is lower than that of polystyrene. However, the

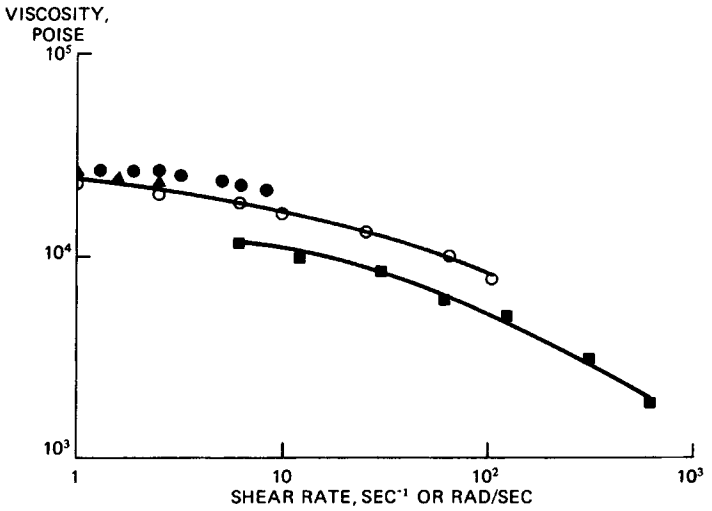


Fig. 11. Rheological properties of cellulose acetate butyrate at 230°C. Symbols as in Fig. 1.

PVC melt is known to be complex, with crystal-like domains which may behave like fairly rigid molecules.

The reasons for these differences are not yet apparent. However, it is obvious that when long, stiff molecules, or domains, are involved, the geometry of the flow in the measuring instrument must be carefully considered. Attempts should not be made to characterize a rotational process with extrusion data. Thus the apparent viscosity in an extruder screw may not be the same as that in a die.

Elastic-modulus values calculated from the two dynamic methods agree quite well, as shown in the figures. The theory and methods of calculation are straightforward. However, such values calculated from normal forces, die swell, and end effects do not agree well, probably because the theories relating these measurements to a modulus are inadequate.

The testing reported here shows that viscosity measurements on polymer melts by these four methods—Instron capillary rheometer, rotating cone and plate, oscillation of cone and plate, and ERD eccentric rotating disks—produce the same results, provided that the following conditions are met:

(1) Measurements are made within the appropriate operating range of each method.

(2) Results are compared at the same shear rate in reciprocal sec and frequency in rad/sec.

(3) Strain amplitudes are about one (or less) for dynamic measurements.

(4) Results are calculated on the basis of the same model, preferably the Maxwell system of additive strains of viscous and elastic components.

(5) Long, very stiff molecules are not involved.

The correlations observed here have also been observed by several other workers in this laboratory and by workers in other laboratories within the company. It is interesting to speculate on what these correlations might tell us about flow mechanisms and the structures of flexible- and rigid-chain polymers; about plasticized or antiplasticized systems; about polymers filled with various types of pigments, pigments of different consistency, and pigments of different shapes (spheres, rods, plates); about different degrees of interaction, such as reinforcing versus nonreinforcing pigments; and about polymer blends.

The authors acknowledge the helpful discussions with Professor D. C. Bogue of the University of Tennessee, Knoxville, and Dr. L. D. Moore and Mr. C. R. Crim of the Tennessee Eastman Research Laboratories.

## APPENDIX A

Derivation of the equations for calculating the parameters $G_m$ and $\eta_m$ for the Maxwell model have caused some problems for rheologists, so the methods are summarized here. Equations for the Voigt parameters $G_v$ and $\eta_v$ can be derived similarly. Clearly, $G_m$ and $\eta_m$ are not $G'$ and $\eta'$ but the values of the modulus and the viscosity of the elements of the model and are assumed constant at a constant frequency $\omega$. This requirement meets experimental conditions in most cases. Also $\delta$ is constant at constant $\omega$. However, $G_m$, $\eta_m$, and $\delta$ can change with a frequency change, just as steady-state viscosity changes with a shear-rate change.

The equation for the Maxwell model is

$$\frac{d\gamma_t}{dt} = \frac{dS_t/dt}{G_m} + \frac{S_t}{\eta_m} \tag{1}$$

where $\gamma_t$ and $S_t$ are the strain and stress at any time ($t$).

For sinusoidal deformation, the following equations can be used:

$$\gamma_t = \gamma_0 \sin(\omega t) \tag{2a}$$

$$\frac{d\gamma_t}{dt} = \gamma_0\omega \cos(\omega t) \tag{2b}$$

$$S_t = S_0 \sin(\omega t + \delta) \tag{2c}$$

$$\frac{dS_t}{dt} = S_0\omega \cos(\omega t + \delta) \tag{2d}$$

where $\gamma_0$ and $S_0$ are the maximum amplitudes of the strain and stress curves, and $\delta$ is the phase angle by which $S_0$ leads $\gamma_0$.

By combining eqs. (2b), (2c), and (2d) with eq. (1), we get

$$\omega\gamma_0 \cos(\omega t) = \frac{\omega S_0 \cos(\omega t + \delta)}{G_m} + \frac{S_0 \sin(\omega t + \delta)}{\eta_m} \tag{3}$$

Since these equations hold for any $t$ (providing, of course, that $t$ is large enough so that the sinusoidal deformation has reached an equilibrium behavior), we can choose $t$ so that $(\omega t + \delta) = 0$; thus, $\omega t = -\delta$ and $\cos(-\delta) = \cos\delta$. Therefore,

$$\omega\gamma_0 \cos\delta = S_0\omega/G_m + 0 \qquad \text{and} \qquad G_m = (S_0/\gamma_0)\,(1/\cos\delta) \tag{4}$$

Likewise, we can set $\omega t + \delta = 90°$, so that $\omega t = 90° - \delta$ and $\cos(90° - \delta) = \sin\delta$, then

$$\omega\gamma_0 \sin\delta = 0 + S_0/\eta_m \qquad \text{and} \qquad \eta_m = (S_0/\gamma_0\omega)\,(1/\sin\delta) \tag{5}$$

We can also set $\omega t = 90°$ and get

$$\tan\delta = G_m/\omega\eta_m = 1/\omega\tau_m \tag{6}$$

To check this derivation another way, we can take the equation for the Maxwell model and convert it to the form

$$\omega\gamma_0 \cos\omega t = \frac{dS/dt}{G_m} + \frac{S}{G_m\tau}$$

Solving for $S$ by integration and letting $t$ be large enough to provide an equilibrium sine curve, we get

$$S = \gamma_0\left(\frac{G_m\omega^2\tau_m^2}{\omega^2\tau_m^2 + 1}\sin(\omega t) + \frac{G_m\omega\tau_m}{\omega^2\tau_m^2 + 1}\cos(\omega t)\right) \tag{7}$$

Substituting the values for $G_m$ and $\tau_m$ from eqs. (4) and (6) with no constraints on $t$, we get

$$S_t = S_0 \sin(\omega t + \delta)$$

which is identical to eq. (2c).

## APPENDIX B

The derivation of equations for calculating Maxwell constants from ERD measurements is as follows[3]:

$$\eta_v = F_y h/\omega\pi R^2 a \qquad \text{and} \qquad G_v = F_x h/\pi R^2 a \tag{8}$$

(these symbols are defined in the text and the glossary, Appendix C. Also,

$$\eta_v = (S_0/\gamma_0\omega)\sin\delta \qquad \text{and} \qquad \eta_m = S_0/\gamma_0\omega \sin\delta \tag{9}$$

By combining eqs. (8) and (9), we get

$$\omega\eta_v/G_v = F_y/F_x = \omega\tau_v = \tan\delta \tag{10}$$

and

$$\delta = \tan^{-1}(F_y/F_x) \tag{11}$$

Combining with eq. (9) gives

$$\eta_m = \eta_v/\sin^2\delta \tag{12}$$

Combining eqs. (12), (8), and (11) gives

$$\eta_m = \frac{F_y h}{\omega\pi R^2 a \sin^2 \tan^{-1}(F_y/F_x)} \tag{13}$$

Similarly,

$$G_m = \frac{F_x h}{\pi R^2 a \cos^2 \tan^{-1}(F_y/F_x)} \tag{14}$$

## APPENDIX C: GLOSSARY OF SYMBOLS

| | |
|---|---|
| $S, \dot{S}, S_t, S_0$ | shear stress, derivative of shear stress, shear stress at time $t$, peak stress in a sinusoidal deformation |
| $\gamma, \dot{\gamma}, \gamma_t, \gamma_0$ | strain, rate of strain, strain at time $t$, peak strain in a sinusoidal deformation |
| $\eta, \eta_m, \eta_v$ | viscosity, viscosity of Maxwell element, viscosity of Voigt element |
| $\eta^*, [\eta^*]$ | complex viscosity, absolute value of complex viscosity |
| $\eta', \eta''$ | real and imaginary parts of complex viscosity |
| $G, G_m, G_v$ | modulus, modulus of Maxwell element, modulus of Voigt element |
| $G^*, [G^*]$ | complex modulus, absolute value of complex modulus |
| $G', G''$ | real and imaginary parts of complex modulus |
| $\tau$ | relaxation time $\eta/G$ |
| $\delta$ | difference in phase between stress and strain in sinusoidal dynamic plots |
| $t$ | time |
| $T$ | temperature |
| $F_x, F_y, F_z$ | forces measured in $x$ direction, $y$ direction, and $z$ direction |
| $h$ | distance between platens (Gap) |
| $a$ | distance of axis offset between platens |
| $\omega$ | frequency (rad/sec) |
| $N_1, N_2$ | first and second normal stress differences |

## References

1. J. D. Ferry, *Viscoelastic Properties of Polymers,* 2nd ed., Wiley, New York, 1970, pp. 60, 61.
2. J. J. Benbow, F. N. Cogswell, and M. M. Cross, *Rheol. Acta,* **15,** 231 (1976).
3. C. W. Macosko and W. M. Davis, *Rheol. Acta,* **13,** 814 (1974).
4. F. Bueche, *Physical Properties of Polymers,* Wiley, New York, 1962, pp. 216–224.
5. C. Bonnebat and A. J. Devries, *Polym. Eng. Sci.,* **18,** 824 (1978).

Received November 30, 1979